Studies in Digital Beamforming for Adaptive Arrays

by

Peter J. McLane
Cecilia Chan
Jason Duggan

Department of Electrical Engineering

Queen's University at Kingston
Kingston, Ontario, Canada

Studies in Digital Beamforming for Adaptive Arrays

by

Peter J. McLane
Cecilia Chan
Jason Duggan

Department of Electrical and Computer Engineering
Queen's University
Kingston, Ontario

October 23, 1997

Final Report
Part B
Communications Research Centre/Queen's University Agreement on
On-Board Processing Via Future Communications Satellites, November 1995.

Abstract

This report is the final report part B on the CRC/Queen's Agreement on On-board Processing Via Future Communications Satellites. The report is focussed on two issues. We first consider interference resolution for the Uniform Linear Array. This study is intended to clarify the concept of the interference cancellation capability of the Uniform Linear Array. We find that the concept of an array with N_E elements having the ability to cancel N_E-2 interferers must be modified as a function of N_E and of the array architecture.

The second part of the report considers the topic of cyclic beamforming but applied to an offset parabolic reflector antenna structure. Such a structure is the usual one used for satellites in geosynchronous orbit. This study extends the work of Mark Rollins, formerly of CRC, who considered cyclic beamforming for the Linear Array. We find that the convergence problem that exists for such an array carries over the parabolic reflector case.

In future we plan to (i) extend our study on interference resolution to the parabolic reflector case and (ii) to study decision feedback detection algorithms as an access method and also to improve the convergence of cyclic beamforming.

A bibliography on signal processing with adaptive arrays is given at the end of this document.

Table of Contents

Chapter 1

Resolution

It is stated in the literature that a N_E-element array has $N_E - 1$ degrees of freedom which can be used to optimize one desired user and null out $N_E - 2$ interferers [49, 68]. Does this imply that the users can be arbitrarily distributed over the coverage area while acceptable system performance is achieved? Or is there a constraint as to how closely packed or sparsely spread the users have to be? Parolin [54] stated that the user signals can be properly resolved only if they are separated by the proper angular separation. Parolin also stated the usable range of a Uniform Linear Array (ULA) to be $-60°$ to $60°$. However, the issue of how exactly should the interferers and desired user be distributed in order to achieve acceptable system performance is not thoroughly investigated in the literature. It is therefore the goal of this report to investigate the relation between the degrees of freedom and resolution.

In this chapter, the usable range of ULA, the degrees of freedom, how these are related to the antenna resolution, the concerns and possible modifications of the optimum combining solution are examined.

The theory behind the calculations in this chapter as well as a diagram of the ULA can be found in Appendix A.

1.1 Usable Range of Uniform Linear Array

Parolin [54] showed that the Uniform Linear Array (ULA) has poor SINR performance when users are incident close to the end-fire positions. A usable range of the antenna is a range within which any angle of incidence for the desired user, denoted as θ_d, will produce acceptable SINR performance. In other words, for any $\theta_d \in [-x, x]$ where $-x$ and x are the range limits, acceptable SINR performance is guaranteed. Here, acceptable SINR performance is defined as achieving a SINR value within 1 dB of SNR_{ideal} [54]. These will be explained in Section 1.2. Table 1.1 shows the SINR obtained when users are packed to the closest possible limit, which is 18°, for an 8-element array. The SNR_{ideal} for an 8-element array is 21.0721 dB. Thus, the acceptable SINR range is from 20.0721 dB to 21.0721 dB. The SINR drops below the limit (< 20.0721 dB) when $|\theta_d| > 60°$. Therefore, to guarantee acceptable SINR performance, the usable range of a ULA is limited to −60° to 60°.

incident angles of users (°)	SINR (dB) (for θ_d from most negative to positive)						
-59, -41, -23, -5, 13, 31, 49	20.2133	20.4284	20.7115	20.7015	20.6948	20.6538	20.5017
-60, -42, -24, -6, 12, 30, 48	20.1462	20.3684	20.6979	20.7067	20.6886	20.6532	20.5046
-61, -43, -25, -7, 11, 29, 47	20.0694	20.2981	20.6795	20.7119	20.6832	20.6505	20.5047
-62, -44, -26, -8, 10, 28, 46	19.9822	20.2163	20.6558	20.7166	20.6788	20.6460	20.5024
-65, -47, -29, -11, 7, 25, 43	19.6479	19.8872	20.5471	20.7224	20.6739	20.6271	20.4858
-70, -52, -34, -16, 2, 20, 38	18.7757	18.9496	20.2041	20.6721	20.6907	20.6020	20.4499

Table 1.1: SINR performance for $N_E = 8$ using different range limits

1.2 Degrees of Freedom

Compton [49] showed that an N_E-element array has $N_E - 1$ degrees of freedom which can be used to optimize 1 desired signal and null out 0 to $N_E - 2$ interferers at the same time.

In a multi-user system, every signal is in turn treated as a desired user and is resolved by a different set of weights. Thus, the antenna array has to achieve two purposes, namely:

1. to ensure that each individual signal can be properly resolved and optimized; and

2. to null out the interferers.

One issue that has often been neglected in the degrees of freedom discussion is that the antenna array can optimize the 1 desired user and null out the 0 to $N_E - 2$ interferers only if all the users (desired and interfering) are spaced properly. This means that the user signals' incident angles should differ by a minimum angle. Only users separated by the proper resolution can be properly resolved. Otherwise, when the users are too closely packed together, two typical problems will arise:

1. the sidelobes between the users or near the end-fire positions will be extraordinarily high which is undesirable as will be explained in Sections 1.3.2 and 1.3.3; and

2. the nulls or peak of the main lobe cannot be properly placed right at the interferer(s) or desired user, thus degrading SINR performance.

The minimum angle mentioned above is the resolution of the antenna array. The antenna array resolution, θ_r, is defined as the smallest amount of angular separation between the desired signal and the nearest interfering signal, while still achieving a large enough SINR to obtain an acceptable BER performance [54]. According to Parolin, the threshold for the acceptable SINR is 1 dB below SNR_{ideal}. SNR_{ideal} is the SINR achieved when there is no interference. In other words, SINR performance is considered acceptable when $\text{SINR}_{achieved} \in [(\text{SNR}_{ideal} - 1), \text{SNR}_{ideal}]$ where here and below SINR is in dB.

Notice that not only is the SINR performance poor when the users are incident near to the end-fire positions and good when the users are incident closer to broadside. In reality, the SINR achieved differs for the same user distribution pattern when the desired user arrives with different θ_d. Thus, θ_r should be determined using the worst

case scenario to get the lower limit. By simulations, the worst case scenario is found to be when the desired user is the farthest user from broadside.

From Section 1.1, the usable range for ULA is from $-60°$ to $60°$. For large N_E, to utilize the $N_E - 1$ degrees of freedom, a rough estimate for θ_r is $(120/(N_E - 2))°$. That is, when the maximum number of interferers, $N_E - 2$, are evenly distributed over the $120°$ range. This estimate is valid when the desired user is arriving at an angle close to broadside. Figure 1.1 shows the antenna pattern and SINR performance for a 32-element array serving 1 desired user arriving at $0°$ and 30 interferers spread over the $-60°$ to $60°$ range with an angular separation of $(120/(32-2))° = 4°$. However, for large N_E, this estimate has to be modified if the desired user is incident close to the limit of the usable range. This will be examined in more detail in Section 1.2.1. Also, for small N_E, θ_r can be smaller than $(120/(N_E - 2))°$. This will be examined in Section 1.2.2.

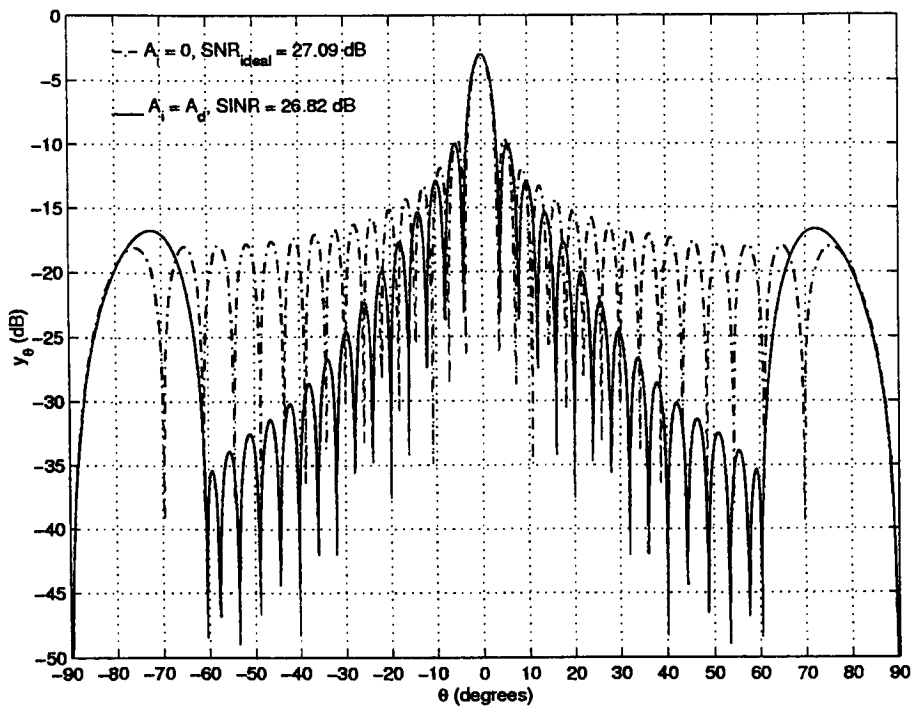

Figure 1.1: Antenna pattern for a 32-element array with 1 desired user, $\theta_d = 0°$, amplitude $= A_d$, and 30 interferers spread over $-60°$ to $60°$, $\Delta\theta_i = (120/(32-2))° = 4°$, amplitude $= A_i$

1.2.1 Resolution and Degrees of Freedom for Large N_E

The estimate of $\theta_r = (120/(N_E - 2))^\circ$ is valid when the desired user is incident close to broadside, i.e., when $|\theta_d|$ is small. However, for large N_E, it has to be modified if the desired user is incident close to the limit of the usable range, i.e. when $\theta_d \approx \pm 60^\circ$.

Recall from Section 1.1 that SINR performance degrades to below the acceptable limit when $|\theta_d| > 60^\circ$. Also, Section 1.2 shows that in order to properly resolve all users, all users must be spaced apart by a minimum angular separation, θ_r. From simulations, it is found that for large N_E, a θ_r larger than $(120/(N_E - 2))^\circ$ is required to ensure acceptable SINR performance when the desired user is arriving close to the usable range limit of $\pm 60^\circ$. The consequence is that it is impossible to fit all the $N_E - 1$ users in the -60° to 60° range with proper angular separation while achieving acceptable SINR performance. As acceptable SINR can only be achieved for large N_E within the 120° range, the only way to allow for larger θ_r is to decrease the number of interferers, N_I.

Table 1.2 shows the maximum number of users (1 desired user + N_I interferers) for different N_E for which SINR performance of within 1 dB SNR_{ideal} is obtained. For $N_E = 10$, $N_E - 1$ users can still be supported. For $N_E = 12$, only $N_E - 2$ users can be supported. For $N_E = 14$ and 16, only $N_E - 3$ users can be supported.

N_E	$1 + N_I$	$\Delta\theta$ (°)	SNR_{ideal} (dB)	SINR (dB) for desired user at $\pm 60^\circ$
10	$9 = N_E - 1$	$120/(9-1) = 15$	22.0412	21.3136
12	$10 = N_E - 2$	$120/(10-1) = 13.33$	22.8330	21.9916
14	$11 = N_E - 3$	$120/(11-1) = 12$	23.5025	23.1216
16	$13 = N_E - 3$	$120/(13-1) = 10$	24.0824	23.6283

Table 1.2: Maximum number of users vs. different N_E

In other words, for large N_E, if a SINR of within 1 dB of SNR_{ideal} is desired, the $N_E - 1$ degrees of freedom cannot be fully utilized.

In light of this, what then is the gain for using antenna arrays of more elements when the same maximum number of users can be served with an antenna array of fewer elements? The answer is that for the same maximum number of users, a higher-

N_E-element array can achieve higher overall SINR. Although the maximum number of users that can be supported versus N_E is suffering from diminishing returns, using higher N_E can nonetheless provide better SINR performance.

1.2.2 Resolution and Degrees of Freedom for Small N_E

For small N_E, θ_r can be smaller than $(120/(N_E - 2))^\circ$. For example, for $N_E = 8$, the required SINR of within 1 dB of the SNR_{ideal} can be achieved using an angular separation of 18° instead of $(120/(8-2))^\circ = 20^\circ$ even when the desired user is incident right at the usable range limit of ±60°. Thus, for small N_E, θ_r is smaller than the rough estimate mentioned above. Nevertheless, the degrees of freedom statement is indisputable in that an N_E-element antenna array can, at most, optimize 1 desired user and null out $N_E - 2$ interferers. In other words, from our simulations, it is shown that when $120^\circ/\theta_r \geq (N_E - 2)$, the ULA can still support only 1 desired user and $N_E - 2$ interferers.

From the discussions in Sections 1.2.1 and 1.2.2, it is clear that although a N_E-element array does have $N_E - 1$ degrees of freedom which can be used to optimize 1 desired user and, at most, null out $N_E - 2$ interferers, in light of system performance, the $N_E - 1$ degrees of freedom cannot always be utilized. Rather, the degrees of freedom statement serves as an upper bound for the maximum number of users supportable by an antenna array.

1.3 Issues of Concern and Possible Improvements

1.3.1 User Distribution Pattern

From Section 1.2.1, θ_r for large N_E has to be greater than or equal to $(120/(N_E - 2))^\circ$ in order to achieve acceptable SINR performance. Thus, the only possible distribution for the users is to have equal angular separation over the −60° to 60° range. However, for small N_E, θ_r can be smaller than $(120/(N_E - 2))^\circ$ as shown in Section 1.2.2. Thus, there are more than one possible distribution patterns for the users. Although the

resultant SINR for users separated by θ_r is always within the acceptable 1 dB range, different user distributions do result in different SINR performance. Moreover, other performance parameters, such as the peak-to-sidelobe ratio as well as the heights of the sidelobes, do change with different distributions. In other words, it is possible to find a distribution more preferable than others with regards to different constraints. Two examples of a 8-element array serving 1 desired user arriving at $\theta_d = 0°$ and 6 interfering users distributed differently are shown in Figures 1.2 and 1.3. It is to be noted that for the case of a non-uniform distribution of interferers, as in Figure 1.3, poorer sidelobe performance, such as low peak-to-sidelobe ratio or high sidelobes at the end-fire positions, is the result. These points will be explained in further detail in Sections 1.3.2 and 1.3.3.

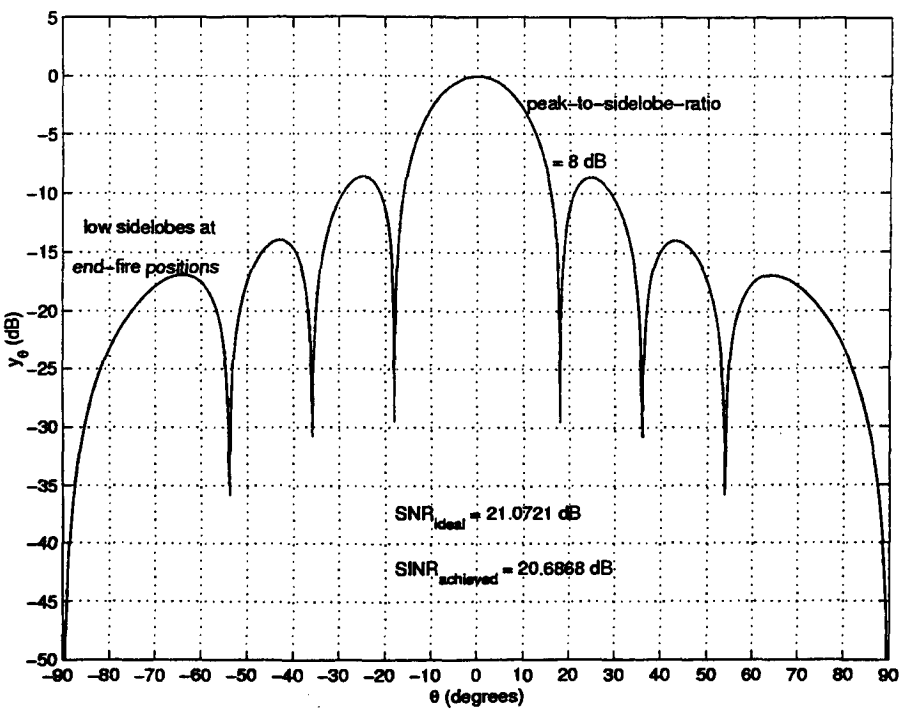

Figure 1.2: Antenna pattern for a 8-element array with 1 desired user, $\theta_d = 0°$, and 6 interferers at $-54°, -36°, -18°, 18°, 36°, 54°$

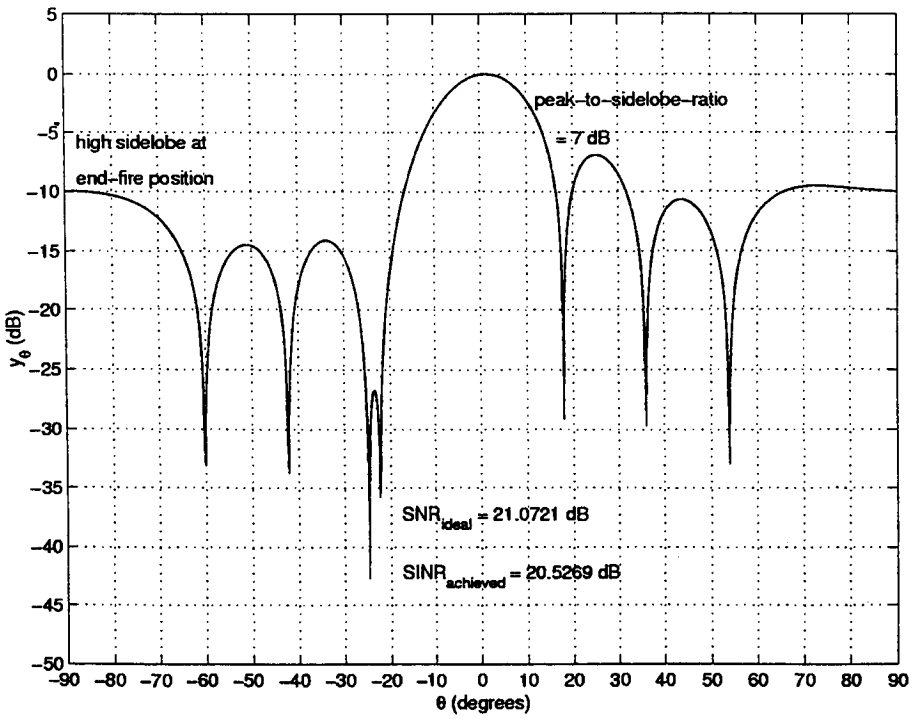

Figure 1.3: Antenna pattern for a 8-element array with 1 desired user, $\theta_d = 0°$, and 6 interferers at $-60°, -42°, -24°, 18°, 36°, 54°$

1.3.2 Peak-to-Sidelobe Ratio

One problem for many of the resultant antenna patterns is that although a very high main lobe is pointed at the desired user and very deep nulls are pointed at the interferers, the magnitudes of the sidelobes are relatively high. The Peak-to-Sidelobe Ratio, PSLR, is defined as the ratio of the peak of the main lobe to the peaks of the closest sidelobes. Figure 1.4 shows an example for $N_E = 8$, $\theta_d = -60°$. The PSLR achieved is only 6 dB. It is not a problem if all the interferers are stationary and the locations are properly distributed. However, one potential danger is that if any one of the interferers is misaligned. Then, it would be right at the peak of the sidelobe instead of at the deep null. As the magnitude of the sidelobe is quite high, the interfering signal will be passed through without much attenuation. Thus, the antenna pattern is not very desirable.

In reality, all that is necessary is to have a fairly deep null placed at each interferer

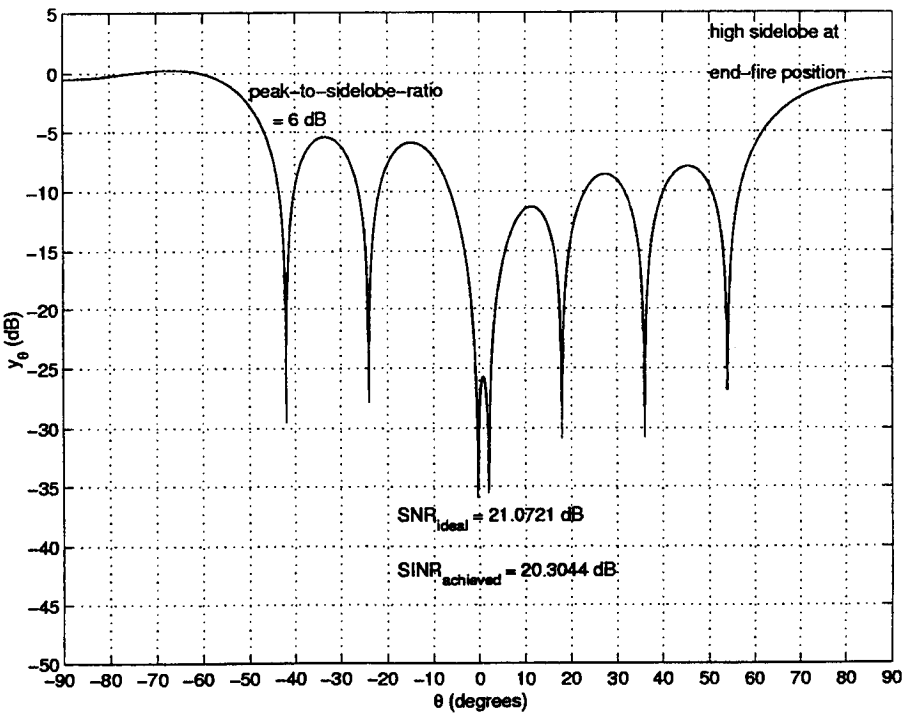

Figure 1.4: Antenna pattern for a 8-element array with 1 desired user, $\theta_d = -60°$, and 6 interferers at $-42°, -24°, 0°, 18°, 36°, 54°$

and also fairly low magnitudes for all sidelobes. In that case, if the nulls are pointed right at the interferers, a good antenna pattern will certainly be obtained. Nevertheless, if there is a slight misalignment of the interfering signal, the low sidelobes will still provide sufficient attenuation to prevent severe distortion to the desired signal.

It is therefore recommended to maintain a minimum of 10 dB difference between the peaks of the main lobe to the sidelobes. In other words, a PSLR of 10 dB is desirable.

1.3.3 Sidelobes Near the End-fire Positions

Another concern about the simulation results is that the sidelobes near the end-fire positions are quite high. For example, in Figure 1.4, the sidelobe at 60° is almost as high as the sidelobe at −60° where the desired user is incident. This is a similar concern as that of the peak-to-sidelobe ratio. Based on the same argument, it is

desirable to maintain all sidelobes, including the ones at the two ends, to be at least 10 dB below the peak of the main lobe.

1.3.4 Solution - Optimization using Non-linear Programming

One way to achieve this recommendation is to use non-linear programming. Presently, the optimum combining theory provides an antenna pattern where deep nulls are pointed at the interferers. Yet little is done to the magnitudes of the other sidelobes. Non-linear programming can be employed to modify the optimum combining solution to take the sidelobe problems into account. Also, depending on the complexity of the solution, an optimum solution may be obtained to take into account the performance differences for different user distributions as well. More work must be put in to investigate the feasibility of this approach.

1.4 Conclusion

1. The usable range of the Uniform Linear Array (ULA) is $-60°$ to $60°$.

2. The simple formula for the minimum angular separation between users, $(120/N_I)°$, where $N_I = N_E - 2$, is accurate as a upper bound for small N_E. For large N_E, N_I must be reduced to achieve a SINR that is within 1 dB of the SNR_{ideal}.

3. If the distribution of interferers is not uniform around the desired user, poorer sidelobe performance (e.g., low peak-to-sidelobe ratio (PSLR), high sidelobes at end-fire positions) is the result.

4. An antenna weight algorithm that optimizes SINR subject to a constraint in PSLR will be studied.

Chapter 2

Cyclic Beamforming Algorithms on a Multiple Beam Antenna

2.1 Introduction and Overview

This chapter considers cyclic beamforming algorithms. Cyclic beamforming algorithms are a class of *blind spatial filtering algorithms* which exploit *property restoral* techniques to restore known properties of the desired signal in the output signal of the array. The key advantage of these blind spatial filtering algorithms is that they don't require a training signal which takes up valuable bandwidth and power resources. There are two property restoral approaches that have been suggested in the literature. The first is the constant modulus algorithm which takes advantage of the low modulus variation of most communication signals. The second property exploited in property restoral algorithms has been *cyclostationarity.* There are many communication signals which exhibit cyclostationarity and this cyclostationarity implies that the signal is *spectrally self-coherent.* In other words, many communication signals are highly correlated with frequency shifted (and possibly conjugated) versions of themselves. Therefore by properly weighting and summing up frequency-shifted versions of the received signal, a desired signal may be extracted from an environment of spectrally incoherent interference.

Cyclic beamforming algorithms are not without their disadvantages and limitations. First of all, the cyclic beamforming algorithms suggested to date either suffer

from a slow convergence rate or a large number of computations. The other key disadvantage of cyclic beamforming algorithms is that they impose limitations on the modulation techniques employed. Certain modulation techniques exhibit more cyclostationarity than others. Despite these disadvantages and limitations, cyclic beamforming algorithms are very interesting. These algorithms are a fairly recent addition to the field of adaptive beamforming and there is still a great deal of room for improvement and innovation.

This chapter focuses on the use of cyclic beamforming algorithms for a multiple beam antenna. Before exhibiting the performance of a cyclic beamforming algorithm on a MBA this chapter will discuss the theory behind cyclostationary signal analysis, and then introduce a number of cyclic blind spatial filtering algorithms which have been proposed in the literature.

2.2 Cyclostationary Signal Analysis

The theory of cyclostationary signal analysis has largely been developed by William A. Gardner and his graduate students. Gardner's 1987 text "Statistical Spectral Analysis: A Non-Probabilistic Theory" [30] was the first full development of the non-statistical theory of cyclostationary time-series. In addition, Gardner has written an excellent tutorial paper on cyclostationary signals titled "Exploitation of Spectral Redundancy in Cyclostationary Signals" [38] which was published in the April 1991 edition of IEEE Signal Processing Magazine. More recently, Gardner has edited the book "Cyclostationarity in Communications and Signal Processing" [31] in 1993. This book covers some of the most recent research in the field of cyclostationary signal processing. In this thesis the non-statistical version of the theory of cyclostationarity, as developed by Gardner [30, 31, 33, 34, 35, 36, 38], will be used. Only the key definitions and ideas of cyclostationary signal processing will be presented. The reader is referred to these other treatments for greater detail.

The key quantity in this chapter is the *cyclic autocorrelation function (CAF)* of

$x(t)$ defined by

$$R_{xx}^{\alpha}(\tau) = \left\langle x(t+\tau/2)\, x^*(t-\tau/2) e^{-j2\pi\alpha t} \right\rangle_{\infty} \tag{2.1}$$

where τ is a time lag, α is a value called the *cycle frequency* and the infinite-duration time-averaging operation has been used

$$< \cdot >_{\infty} = \lim_{Z\to\infty} \frac{1}{2Z} \int_{-Z}^{Z} (\cdot)\, dt. \tag{2.2}$$

We may also define the *cyclic conjugate-correlation function* of $x(t)$ defined by

$$R_{xx^*}^{\alpha}(\tau) = \left\langle x(t+\tau/2) x(t-\tau/2) e^{-j2\pi\alpha t} \right\rangle_{\infty}. \tag{2.3}$$

The CAF is a quadratic nonlinear transformation. If the CAF of a time-series $x(t)$ is nonzero for some value α and time lag τ then the signal $x(t)$ is said to be *second-order cyclostationary.* Note that for $\alpha = 0$, the CAF reduces to the conventional autocorrelation function which is

$$R_{xx}^{0}(\tau) = R_{xx}(\tau) = \langle x(t+\tau/2)\, x^*(t-\tau/2) \rangle_{\infty}. \tag{2.4}$$

$R_{xx}^{\alpha}(\tau)$ may be thought of as a generalization of the autocorrelation function where a cyclic weighting factor $e^{-j2\pi\alpha t}$ is included. Note that the CAF may be rewritten as

$$R_{xx}^{\alpha}(\tau) = \left\langle \left[x(t+\tau/2) e^{-j\pi\alpha(t+\tau/2)}\right] \left[x(t-\tau/2) e^{j\pi\alpha(t-\tau/2)}\right]^* \right\rangle_{\infty}. \tag{2.5}$$

By defining the two functions $u(t)$ and $v(t)$ by

$$u(t) = x(t) e^{-j\pi\alpha t} \tag{2.6}$$

$$v(t) = x(t) e^{+j\pi\alpha t} \tag{2.7}$$

equation (2.5) may be written as a conventional cross-correlation function

$$R_{xx}^{\alpha}(\tau) = R_{uv}(\tau) = \langle u(t+\tau/2)\, v^*(t-\tau/2) \rangle_{\infty}. \tag{2.8}$$

When a signal is multiplied by $e^{+j\pi\alpha t}$ it is translated in frequency by $\alpha/2$. Therefore $u(t)$ and $v(t)$ represent frequency shifted versions of $x(t)$ by $-\alpha/2$ and $\alpha/2$

respectively. Since the CAF may be written as a cross-correlation function of $u(t)$ and $v(t)$ it follows that the CAF of $x(t)$ is nonzero only if $u(t)$ and $v(t)$ are correlated. Therefore $x(t)$ is second-order cyclostationary if and only if $x(t)$ exhibits *spectral self-coherence for frequency separation* α. Note that if the cyclic conjugate-correlation function is nonzero for some value of α and τ then $x(t)$ is said to be *spectrally conjugate self-coherent for frequency separation* α.

The introduction of $u(t)$ and $v(t)$ also allows us to introduce an appropriate normalization of the CAF. If $u(t)$ and $v(t)$ are zero mean then the cross-correlation function defined above is equivalent to the cross-covariance function

$$\begin{aligned} C_{uv}(\tau) &= \langle [u(t+\tau/2) - < u(t+\tau/2) >_\infty] \\ &\quad [v(t-\tau/2) - < v(t-\tau/2) >_\infty]^* \rangle_\infty \qquad (2.9) \\ &= R_{uv}(\tau). \qquad (2.10) \end{aligned}$$

The appropriate normalization factor is the geometric mean of the two temporal variances

$$\begin{aligned} C_{uu}(0) &= \left\langle |u(t)|^2 \right\rangle_\infty = R_{xx}(0) \qquad (2.11) \\ C_{vv}(0) &= \left\langle |v(t)|^2 \right\rangle_\infty = R_{xx}(0). \qquad (2.12) \end{aligned}$$

Therefore the normalized quantity called the *cyclic temporal correlation function* (also called the *spectral self-coherence function* in the literature) is defined by

$$\gamma_{xx}^{\alpha}(\tau) = \frac{C_{uv}(\tau)}{\sqrt{C_u(0)C_v(0)}} = \frac{R_{xx}^{\alpha}(\tau)}{R_{xx}(0)}. \qquad (2.13)$$

The magnitude of the cyclic temporal correlation function, $|\gamma_{xx}^{\alpha}(\tau)|$, varies between 0 and 1 and represents the strength of the correlation. It is referred to as the *feature strength* and it is an important quantity in determining the convergence of cyclic adaptive beamforming algorithms.

Before proceeding to a discussion of cyclic blind spatial filtering algorithms one modification of the cyclic autocorrelation function definition has to be made for the

situation where we have a vector of data as we do in array signal processing. If there are N_E elements in the array then the CAF is defined as an $N_E \times N_E$ matrix

$$\mathbf{R}^{\alpha}_{\mathbf{xx}}(\tau) = \left\langle \mathbf{x}(t+\tau/2)\mathbf{x}^{\dagger}(t-\tau/2)e^{-j2\pi\alpha t}\right\rangle_{\infty}, \tag{2.14}$$

and the cyclic conjugate-correlation function of $\mathbf{x}(t)$ is defined as

$$\mathbf{R}^{\alpha}_{\mathbf{xx}^*}(\tau) = \left\langle \mathbf{x}(t+\tau/2)\mathbf{x}^{T}(t-\tau/2)e^{-j2\pi\alpha t}\right\rangle_{\infty}. \tag{2.15}$$

2.3 Cyclic Blind Spatial Filtering Algorithms

There are many cyclic blind spatial filtering algorithms that have been introduced in the literature in the past few years. In the next section a brief survey of these algorithms will be presented and then this will be followed by a more detailed discussion of one of the simplest of these algorithms, called LS-SCORE. LS-SCORE is an algorithm in the spirit of the reference signal based algorithms such as direct matrix inversion (DMI). The only difference is that LS-SCORE gets its reference signal blindly. In other words, LS-SCORE extracts a reference signal that is correlated with the desired user and uncorrelated with the interferers from the incoming data. Other than that LS-SCORE is exactly like any other reference signal based algorithm.

2.3.1 Cyclic Blind Spatial Filtering Algorithms - A Brief Overiew

The initial work on cyclic blind spatial filtering algorithms was performed by Gardner, Agee and Schell in the late 1980's [32]. They developed a set of algorithms collectively referred to as the SCORE family of algorithms where SCORE refers to *Spectral Coherence REstoral.* Their basic idea is as follows. A signal which exhibits cyclostationarity is spectrally self-coherent. This spectral self-coherence is degraded by the addition of interference that is not spectrally self-coherent at the same value of frequency shift. So, their approach is to restore the spectral self-coherence of the signal of interest and thus the name Spectral Coherence Restoral. There are three

main SCORE algorithms: Least-Squares SCORE (LS-SCORE), Cross-SCORE, and Auto-SCORE. Each has a different cost function based on some measure of spectral self-coherence at the output of the spatial filter.

Least-squares SCORE [32] uses the familiar least-squares cost function

$$\min_{\mathbf{w}} \langle |y(t) - r(t)| \rangle_T \tag{2.16}$$

where, $y(t) = \mathbf{w}^\dagger \cdot \mathbf{x}(t)$ is the output of the spatial filter, $< \cdot >_T$ denotes time-averaging over the interval $[0, T]$, and $r(t)$ is a reference signal derived from the data and given by

$$r(t) = \mathbf{c}^\dagger \cdot \mathbf{x}^{(*)}(t - \tau) e^{j2\pi\alpha t} \tag{2.17}$$

where $\mathbf{c}$ is a control vector (kept fixed) and the optional conjugation $^{(*)}$ is applied only if conjugate self-coherence is to be restored.

Cross-SCORE [32] maximizes the strength of the *temporal cross-correlation coefficient*, $\left|\gamma_{yr}^{\alpha}(\tau)\right|^2$, between the output signal $y(t)$ and the reference signal $r(t)$ (from equation (2.17)). This is done by adapting both the weight vector $\mathbf{w}$ and the control vector $\mathbf{c}$. The cost function becomes

$$\max_{\mathbf{w},\mathbf{c}} \left|\gamma_{yr}^{\alpha}(\tau)\right|^2 = \max_{\mathbf{w},\mathbf{c}} \frac{\left|\mathbf{w}^\dagger \mathbf{R}_{\mathbf{xx}}^{\alpha}(\tau)\mathbf{c}\right|^2}{\left[\mathbf{w}^\dagger \mathbf{R}_{\mathbf{xx}} \mathbf{w}\right]\left[\mathbf{c}^\dagger \mathbf{R}_{\mathbf{xx}} \mathbf{c}\right]}. \tag{2.18}$$

Cross-SCORE has a better convergence rate than LS-SCORE because the control vector $\mathbf{c}$ is also adapted. This improved convergence rate is achieved at the cost of increased computational complexity.

Unlike LS-SCORE which resembles conventional adaptive algorithms, and Cross-SCORE which is really just an extension of LS-SCORE, Auto-SCORE [32] is a pure property restoral algorithm. Auto-SCORE maximizes the spectral or conjugate self-coherence strength at the output of the beamformer. In other words, the cost function is given by

$$\max_{\mathbf{w}} \left|\gamma_{yy^{(*)}}^{\alpha}(\tau)\right| = \max_{\mathbf{w}} \frac{\left|\mathbf{w}^\dagger \mathbf{R}_{\mathbf{xx}^{(*)}}^{\alpha}(\tau)\mathbf{w}^{(*)}\right|}{\mathbf{w}^\dagger \mathbf{R}_{\mathbf{xx}} \mathbf{w}^{(*)}}. \tag{2.19}$$

One of the disadvantages of the SCORE family of algorithms is their computational complexity. There have been several attempts at achieving an algorithm with a reduced computational cost but similar performance to the SCORE algorithms. Wu and Wong [39, 40] have presented a family of algorithms called CAB, short for *cyclic adaptive beamforming.* CAB is a variant on Cross-SCORE. Instead of maximizing $\left|\gamma_{yr}^{\alpha}(\tau)\right|^2$, CAB attempts to maximize the *cyclic sample correlation* given by $\left|\langle y(t)r^*(t)\rangle_{N_S}\right|^2$. Several different variants on both the CAB and SCORE algorithms have been suggested in the literature with varying computational requirements and rates of convergence.

This section has very briefly gone over a few of the cyclic beamforming algorithms proposed in the literature. There are several more, many of which are variants on the ones discussed above. The next section will go into the LS-SCORE algorithm in more detail. The essential goal of this chapter is to demonstrate that cyclic beamforming will work on a multiple beam antenna. LS-SCORE was the chosen algorithm because it is very similar to the algorithms already discussed and yet it demonstrates the exploitation of the cyclostationarity inherent in the signal. In other words, LS-SCORE is the perfect algorithm to build our understanding upon.

2.3.2 LS-SCORE

In this chapter LS-SCORE is the cyclic adaptive beamforming algorithm which we concentrate our attention upon. As expressed in equation (2.16), LS-SCORE involves a least-squares cost function

$$\min_{\mathbf{w}} \langle |y(t) - r(t)| \rangle_T \tag{2.20}$$

with $r(t)$ as the reference signal given by equation (2.17),

$$r(t) = \mathbf{c}^\dagger \cdot \mathbf{x}^{(*)}(t-\tau)e^{j2\pi\alpha t}. \tag{2.21}$$

The value of the control vector $\mathbf{c}$ is kept fixed as we vary the weights. Recall that the optional conjugation is only used if we are interested in restoring conjugate spectral

coherence. Reference [32] shows that the reference signal contains a component that is correlated with the desired signal and a corruption term that is uncorrelated with both the desired signal and the interference and noise. In fact, [32] goes on to show that the square of the feature strength, $|\gamma_{xx}^{\alpha}(\tau)|^2$, is a measure of the relative strength of $x(t)$ contained within $x^{(*)}(t-\tau)e^{j2\pi\alpha t}$. Let us consider using a direct matrix inversion approach to LS-SCORE with (2.21) as the reference signal. From the incoming data we form the sample correlation matrix,

$$\hat{\mathbf{\Phi}} = \frac{1}{N_p}\sum_{l=1}^{N_p} \mathbf{x}(l)\mathbf{x}^{\dagger}(l) \tag{2.22}$$

and the sample correlation vector,

$$\hat{\mathbf{S}}_{corr} = \frac{1}{N_p}\sum_{l=1}^{N_p} r(l)\mathbf{x}^{*}(l) \tag{2.23}$$

and then form the optimum weights

$$\mathbf{w} = \hat{\mathbf{\Phi}}^{-1}\hat{\mathbf{S}}_{corr}^{*}. \tag{2.24}$$

As the number of samples approaches infinity

$$\begin{aligned} \mathbf{w} &\rightarrow \mathbf{\Phi}^{-1}\mathbf{S}_{corr}^{*} && (2.25)\\ &= \mathbf{\Phi}^{-1}\left\langle \mathbf{x}(t)\,\mathbf{x}^{\dagger}(t-\tau)\,\mathbf{c}\,e^{-j2\pi\alpha t}\right\rangle_{\infty} \\ &= \mathbf{\Phi}^{-1}\,\mathbf{R}_{\mathbf{xx}}^{\alpha}(\tau)\,\mathbf{c}\,e^{-j\pi\alpha\tau}. && (2.26) \end{aligned}$$

Provided the noise and interference are not spectrally coherent at cycle frequency α then

$$\mathbf{R}_{\mathbf{xx}}^{\alpha}(\tau) = \mathbf{u}_d\mathbf{u}_d^{\dagger}R_{dd}^{\alpha}(\tau) \tag{2.27}$$

where $\mathbf{u}_d$ is the steering vector of the desired user and $R_{dd}^{\alpha}(\tau)$ is the cyclic autocorrelation function of the desired user's signal. Therefore,

$$\begin{aligned} \mathbf{w} &\rightarrow \left(\mathbf{u}_d^{\dagger}\,\mathbf{c}\,e^{-j\pi\alpha t}\,R_{dd}^{\alpha}(\tau)\right)\mathbf{\Phi}^{-1}\,\mathbf{u}_d && (2.28)\\ &= \varrho\,\mathbf{\Phi}^{-1}\mathbf{u}_d && (2.29) \end{aligned}$$

where ϱ is a constant. Equation (2.29) indicates that we come to within a scalar constant of the optimum weights. A closer look at the scalar, ϱ, applies a condition that the control vector may not be orthogonal to the steering vector of the desired user. Therefore, since scaling of the weights doesn't change the SINR, we've reached the optimum SINR solution for the weights.

The above development has shown that LS-SCORE approaches the optimum solution. The reference signal in (2.21) contains a component that is correlated with the desired signal and a corruption term which is uncorrelated with both the desired signal, the noise and the interference [32]. As one might suspect the performance of LS-SCORE is poorer than when we have a reference signal supplied to us (via a training signal or separate signalling channel) that is perfectly correlated with the desired user. The advantage is that since the reference signal was derived from the incoming data signal through the exploitation of the cyclostationarity inherent in the desired signal, we don't require a training signal or a separate signalling channel which consume precious bandwidth. In the next section the cyclostationarity inherent in a BPSK signal is examined and this is then followed up with a simulation of LS-SCORE with BPSK signalling.

2.4 Cyclostationarity of BPSK

In the next section the simulation of LS-SCORE performed on a focal fed reflector antenna (a MBA) is described. The simulation is a baseband simulation and the signalling method selected was BPSK. This is equivalent to a PAM signal which takes the form

$$x(t) = \sum_{n=-\infty}^{\infty} a_n p(t - nT_o) \tag{2.30}$$

where $\{a_n = a(nT_o)\}$ is a sequence of random variables and $p(t)$ is a deterministic finite-energy pulse. A square pulse shape has been used in the simulation. Gardner [31] has shown that if we assume that the input sequence $\{a_n\}$ is stationary, uncorrelated and unit power then $x(t)$ exhibits cyclostationarity at $\alpha = \pm m/T_o$ where m

is an integer. Moreover, the feature strength is strongest for $m = 1$ and for $\tau = T_o/2$ (for a square pulse shape). These are termed *baud rate features.* Therefore signals with different baud rates will exhibit cyclostationarity at different values of α and τ. This allows the cyclic adaptive algorithm to distinguish between signals with different baud rates.

A second type of cyclostationarity may be created by offsetting each signal from the center of the reception band. In other words, each user which shares a frequency channel has a unique carrier offset. Gardner, Schell and Murphy state that a signal offset by Δf and with baud rate f_b will exhibit *conjugate spectral coherence* for $\alpha = \pm 2\Delta f \pm m f_b$ where m is an integer [29]. This is maximized for $m = 0$ and at $\tau = 0$. The signal is said to exhibit *carrier rate features.*

The simulation in the next chapter will demonstrate LS-SCORE for both baud and carrier rate features.

2.5 Simulation of LS-SCORE

A baseband simulation of LS-SCORE operating on a MBA was performed. The pulse shape chosen was a square pulse. The antenna has $F = 94.87\lambda$, $a = 54.08\lambda$, and $d_{off} = 70.94\lambda$.* The array consists of 7 feeds in the a hexagonal configuration. Each feed is linearly x-polarized and has $q_E = 3.6$ and $q_H = 2.8$. The feeds are spaced 1λ apart with the center feed displaced from the focal point along the x-axis at a distance of -5.53λ. We have a single desired user and a single interferer. The desired user arrives from 3.0° and has SNR of 10 dB. The interferer arrives from 2.4° and also has a SNR of 10 dB.

Two simulations were performed. The first simulation demonstrated baud rate features, the second carrier rate features. 100 trials were performed. The signals used were mutually independent BPSK waveforms with a square pulse shape and time was normalized to the sampling period. For each user a random bit sequence was generated as was a uniformly distributed initial phase in the range of 0 to 2π.

* The structure of the MBA is given in Figure 2.1 and the hexagonal feed configuration is given on Page 77 of [67].

For the baud rate simulation we let the desired user have a symbol period of 4 samples while the interferer has a symbol period of 5 samples. Therefore, we will set the cycle frequency to $\alpha = 1/T_d = 0.25$ in order to extract the desired signal. T_d represents the symbol period for the desired user's signal. We will set the time lag parameter, τ, to $T_d/2 = 2$. 8000 samples (giving 2000 desired signal symbol periods) were taken for each of the 100 trials.

For the carrier rate simulation we set the symbol period of both users to 4 samples per symbol. This time, each user has a distinct carrier offset. The desired user's carrier offset was selected to be $\Delta f_d = 0.0208$ and that of the interfer was set to $\Delta f_i = 0.0417$. One key point is that in order to take advantage of carrier rate features we must look for conjugate self-coherence. We set the cycle frequency to $\alpha = 2\Delta f_d = 0.0416$ and the time lag $\tau = 0$ in order to extract the desired user's signal. As in the baud rate simulation, 8000 samples were taken for each of the 100 trials.

The reference signal for both simulations was formed using equation (2.17) with the control vector set to $\mathbf{c} = [1\,0\,0 \cdots 0]^T$.

At each sample the received signal vector at the antenna array was determined. This was done by adding up the contribution of the desired signal, the interferer, and the noise. The desired user's and the interferer's received signal across the array were found by multiplying the appropriate BPSK waveform at the sample by the steering vector of the user. The reflector antenna analysis program and reciprocity were used to derive the steering vectors. To generate the received noise vector complex random noise samples were generated using a noise variance of 1. The desired user's signal was added with that of the interferer and the noise samples giving the received signal at the array. With the received signal vector the reference signal was calculated using the appropriate value of cycle frequency, α, and time lag, τ, to extract the desired user's signal. As well, if conjugate self-coherence was being exploited, as it was in the carrier rate simulation, then the optional conjugation was used in equation (2.17).

As the resulting received signal at the array and reference signal were determined

at each sample, the sample correlation matrix and sample correlation vector were updated. Every 40 samples (10 symbols) the optimum weight vector was determined by inverting the sample correlation matrix and then multiplying it by the conjugate of the sample correlation vector. Using these weights the output SINR was calculated.

The results of both the baud rate and the carrier rate simulation are shown in figure (2.2). The convergence of the DMI algorithm is shown in figure 2.3 [67]. The results of the simulation are quite revealing. First of all note that the convergence time of the LS-SCORE algorithm, whether baud or carrier rate features are being exploited, is much longer than that of the DMI algorithm which has a perfect reference signal. Second of all, note that the convergence with carrier rate features is much superior to that with baud rate features. This is due to a much larger feature strength for carrier rate features. Perhaps the most important point to note from these simulations is that cyclic adaptive beamforming algorithms do work on multiple beam antennas and no changes need to be made to the algorithms in order to get them to work. This has only been demonstrated for LS-SCORE but the principle is the same and this fact carries over to other cyclic adaptive beamforming algorithms.

Geometry of the Offset Reflector

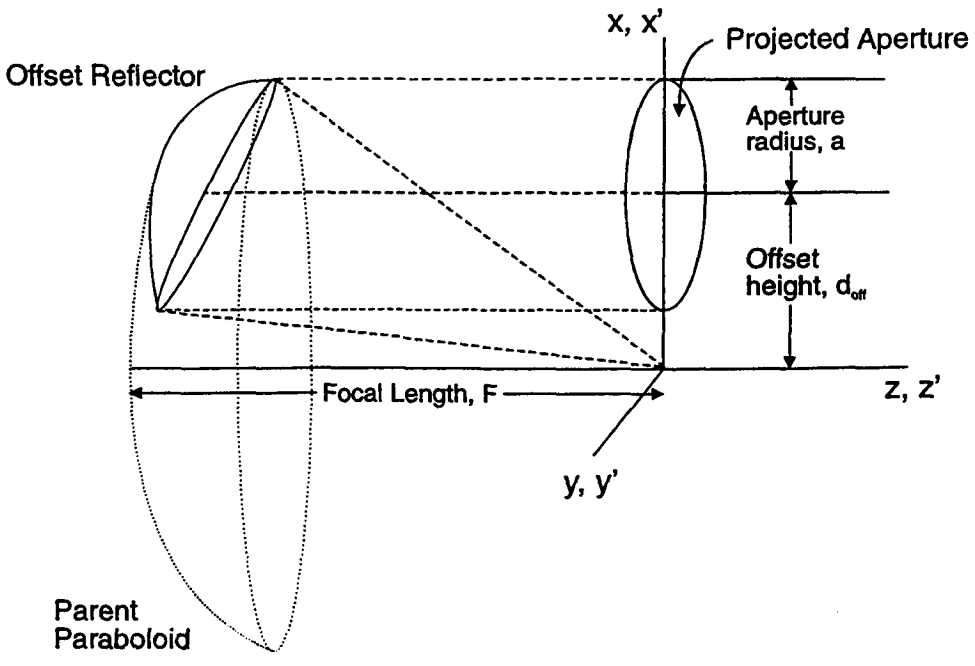

Figure 2.1: 3 dimensional illustration of the geometry of the offset reflector

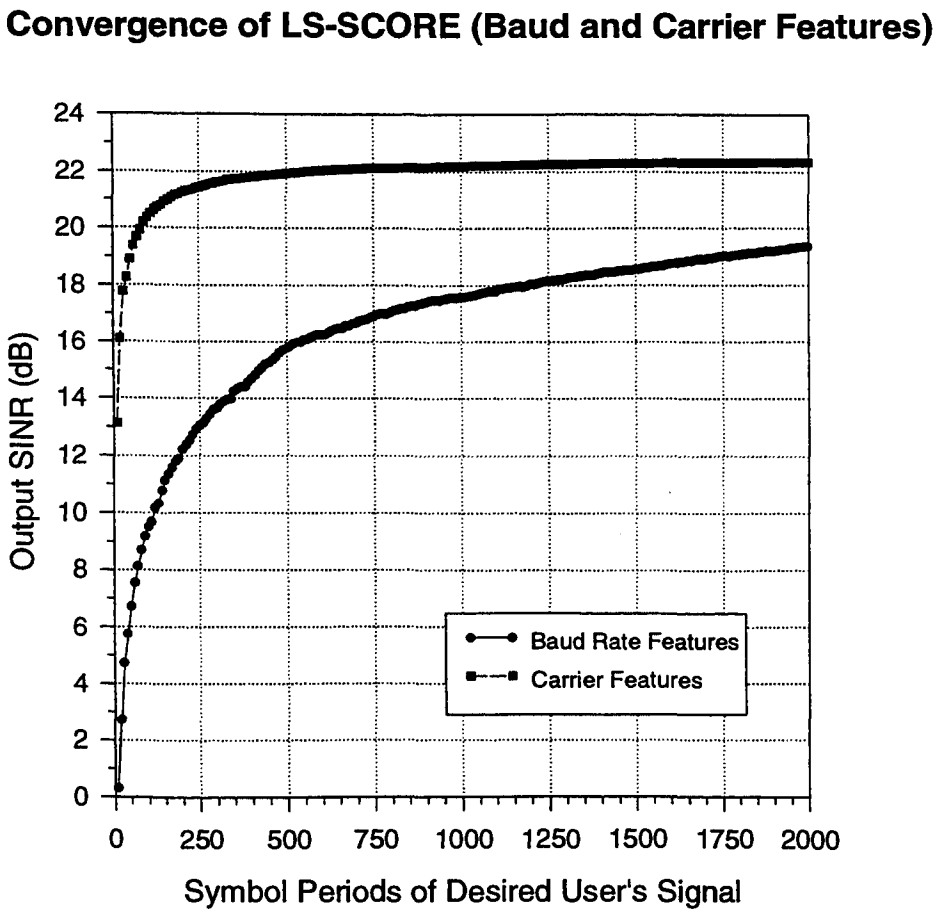

Figure 2.2: Convergence of the LS-SCORE algorithm when performed on a MBA for baud and carrier rate features with a desired user ($\rho_d = 10\,dB, \theta_d = 3.0°$) and a single interfering user ($\rho_1 = 10\,dB, \theta_1 = 2.4°$)

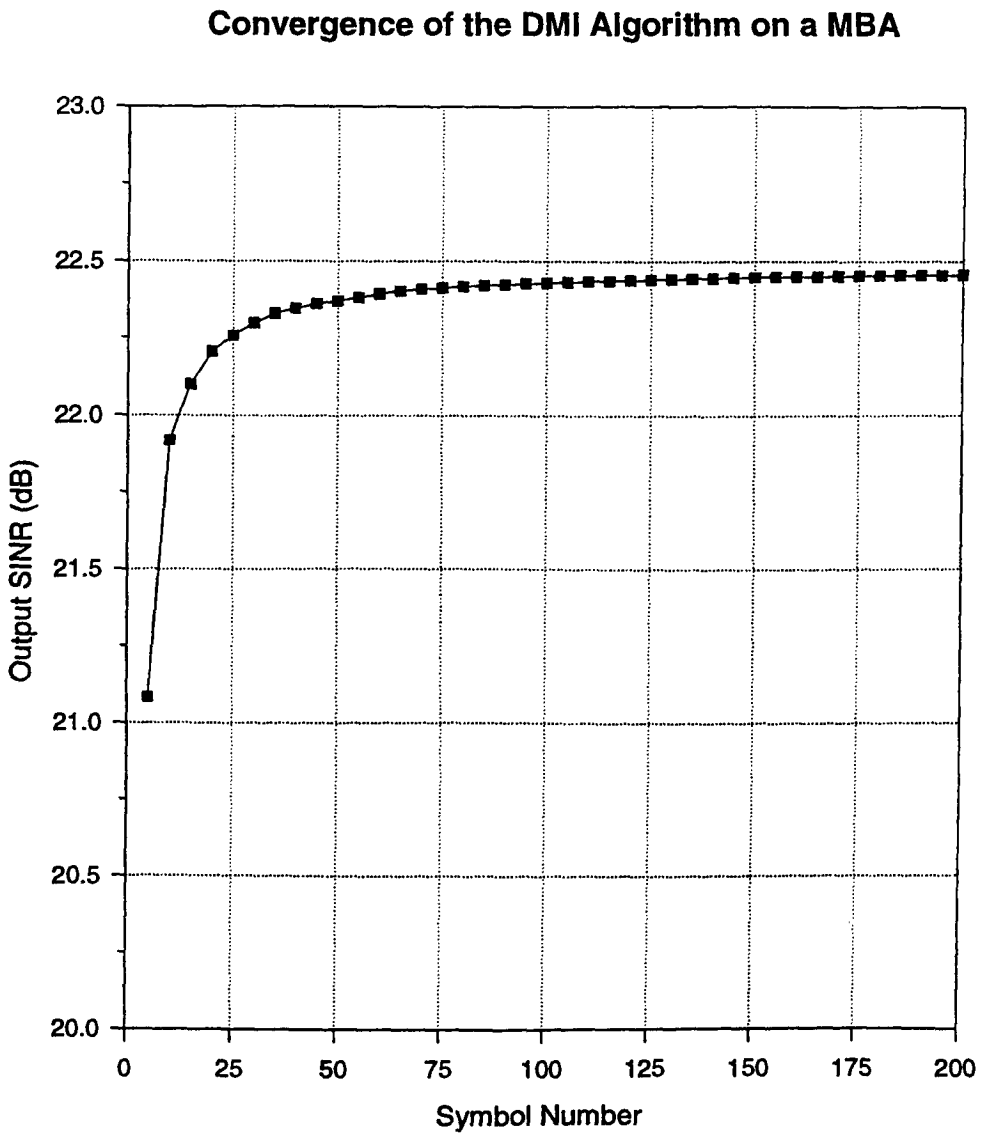

Figure 2.3: Convergence of the DMI algorithm when performed on a MBA (same antenna and feed configuration as in optimum combining demonstration) with a desired user ($\rho_d = 10\,dB, \theta_d = 3.0°$) and a single interfering user ($\rho_1 = 10\,dB, \theta_1 = 2.4°$)

Appendix A

Statistically Optimum Beamforming

The antenna patterns in Chapter 1 are developed by statistically optimum beamforming. In this appendix, the signal model and the Minimum Mean-Square Error algorithm used for the analysis will be discussed.

A.1 Narrow Band Signal Model

The most common Direct Radiating Antenna (DRA), namely, the Uniform Linear Array (ULA), is employed in the analysis and simulations in Chapter 1. ULA refers to the class of antenna arrays with identical antenna elements placed in a line and spaced an equal distance apart [67]. A narrow band signal model is adopted for analysis purposes. Figure A.1 shows a simple ULA of two elements with a desired signal incident at θ_d.

The desired signal arriving at the 2 elements are:

$$x_d(t) = e^{j(2\pi f t+\psi_d)} \tag{A.1}$$

$$x_d(t-\tau) = e^{j(2\pi f(t-\tau)+\psi_d)} \tag{A.2}$$

$$= e^{j(2\pi f t+\psi_d-\phi_d)} \tag{A.3}$$

$$\Rightarrow x_d(t-\tau) = x_d(t)e^{-j\phi_d} \tag{A.4}$$

where τ is the time delay of arrival between the two elements, ϕ_d is the inter-element

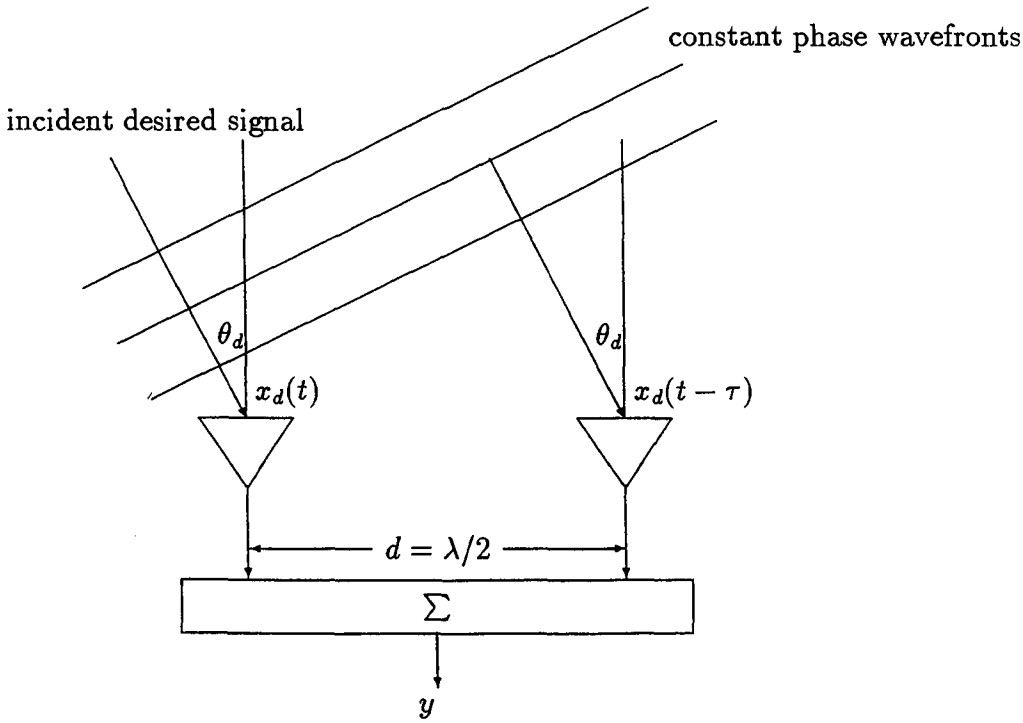

Figure A.1: A ULA with element spacing of $d = \lambda/2$, desired signal incident at θ_d

phase shift of the desired user.

Using vector notation, the received signal vector of the desired user, $\mathbf{x}_d$, is then:

$$\begin{aligned} \mathbf{x}_d &= \begin{bmatrix} x_d(t) \\ x_d(t-\tau) \end{bmatrix} && \text{(A.5)} \\ &= x_d(t) \begin{bmatrix} 1 \\ e^{-j\phi_d} \end{bmatrix} && \text{(A.6)} \\ &= x_d(t)\mathbf{u}_d && \text{(A.7)} \\ &= A_d e^{j\psi_d}\mathbf{u}_d && \text{(A.8)} \end{aligned}$$

where $A_d = e^{j2\pi ft}$, and $\mathbf{u}_d = \begin{bmatrix} 1 \\ e^{-j\phi_d} \end{bmatrix}$ is the steering vector of the desired user.

In the situation under study, besides the one desired user, there are also N_I interfering users and noise, denoted as $\mathbf{x}_n$, in the environment. By similar derivation, each interfering user signal vector, $\mathbf{x}_i$, is represented as:

$$\mathbf{x}_i = A_i e^{j\psi_i}\mathbf{u}_i \qquad \text{(A.9)}$$

By superposition, the overall received signal vector is then:

$$\mathbf{x} = \mathbf{x}_d + \sum_{i=1}^{N_I} \mathbf{x}_i + \mathbf{x}_n \tag{A.10}$$

For beamforming, the signal received at each element is multiplied by an optimum complex weight, and the weighted signals are then summed to form the array output. The antenna pattern, y_θ, is the variation of the antenna output power with the angle of arrival.

$$y_\theta = |\mathbf{w}_{opt}^\dagger \mathbf{u}_\theta| \tag{A.11}$$

where $\mathbf{w}_{opt}$ is the optimum weight vector, and the † symbol denotes Hermitian transpose.

A.2 Minimum Mean-Square Error Algorithm

To find the optimum weight vector, $\mathbf{w}_{opt}$, the Minimum Mean-Square Error (MSE) algorithm employs a reference signal, r, that is perfectly correlated with the desired signal and uncorrelated with the interfering signals and noise. Setting $\psi_r = \psi_d$,

$$r = A_r e^{j\psi_d} \tag{A.12}$$

The error signal, ε, is defined as:

$$\varepsilon = r - \mathbf{w}^\dagger \mathbf{x} \tag{A.13}$$

By Orthogonality Principle:

$$E\{|\varepsilon|^2\} = \text{minimum} \tag{A.14}$$

when

$$E\{\varepsilon \mathbf{x}^\dagger\} = 0 \tag{A.15}$$

That is,

$$E\{r\mathbf{x}^\dagger - \mathbf{w}^\dagger \mathbf{x}\mathbf{x}^\dagger\} = 0 \tag{A.16}$$

$$\Rightarrow E\{r\mathbf{x}^\dagger\} = \mathbf{w}^\dagger E\{\mathbf{x}\mathbf{x}^\dagger\} \tag{A.17}$$

Define the correlation matrix, $\mathbf{\Phi}$, and the correlation vector, $\mathbf{S}_{corr}$, to be:

$$\begin{aligned}
\mathbf{\Phi} &= E\{\mathbf{x}\mathbf{x}^\dagger\} && \text{(A.18)}\\
&= E\{(\mathbf{x}_d + \sum_{i=1}^{N_I} \mathbf{x}_i + \mathbf{x}_n)(\mathbf{x}_d^\dagger + \sum_{i=1}^{N_I} \mathbf{x}_i^\dagger + \mathbf{x}_n^\dagger)\} && \text{(A.19)}\\
&= E\{\mathbf{x}_d\mathbf{x}_d^\dagger\} + \sum_{i=1}^{N_I} E\{\mathbf{x}_i\mathbf{x}_i^\dagger\} + E\{\mathbf{x}_n\mathbf{x}_n^\dagger\} && \text{(A.20)}\\
&= A_d^2\mathbf{u}_d\mathbf{u}_d^\dagger + \sum_{i=1}^{N_I} A_i^2\mathbf{u}_i\mathbf{u}_i^\dagger + \sigma_n^2\mathbf{I} && \text{(A.21)}\\
\mathbf{S}_{corr} &= E\{r\mathbf{x}^*\} && \text{(A.22)}\\
&= E\{r\mathbf{x}_d^*\} && \text{(A.23)}\\
&= A_d A_r \mathbf{u}_d^* && \text{(A.24)}
\end{aligned}$$

Then, the minimum MSE solution is:

$$\mathbf{w}_{opt} = \mathbf{\Phi}^{-1}\mathbf{S}_{corr}^* \qquad \text{(A.25)}$$

Bibliography

[1] B.D. Van Veen, and K.M. Buckley. Beamforming: A Versatile Approach to Spatial Filtering. *IEEE ASSP Magazine*, pp. 4-24, April 1988.

[2] J. Marr. A selected bibliography on adaptive antenna arrays. *IEEE Transactions on Aerospace and Electronic Systems*, Vol AES-22, pp. 781-798, November 1986.

[3] I.S. Reed, J.D. Mallett, and L.E. Brennan. Rapid Convergence Rate in Adaptive Arrays. *IEEE Transactions on Aerospace and Electronic Systems*, Vol. 10, No. 6, pp. 853-863, November, 1974.

[4] J.H. Winters. Optimum Combining for Indoor Radio Systems with Multiple Users. *IEEE Transactions on Communications*, Vol. 35, No. 11, November 1987.

[5] B. Widrow, J. McCool, and M. Ball. The Complex LMS Algorithm. *IEEE Proceedings*, pp.719-720, April, 1975.

[6] W.F. Gabriel. Adaptive Arrays- An Introduction. *IEEE Proceedings*, Vol. 64, No. 2, pp. 239-272, February, 1976.

[7] S.M. Yuen. Exact Least Squares Adaptive Beamforming Using an Orthogonalization Network. *IEEE Transactions on Aerospace and Electronic Systems*, Vol. 27, No. 2, pp. 311-330, March, 1991.

[8] W.F. Gabriel. Adaptive Processing Array Systems. *IEEE Proceedings*, Vol. 80, No. 1, pp. 152-162, January, 1992.

[9] Z. Raida. Steering an Adaptive Antenna Array by the Simplified Kalman Filter. *IEEE Transactions on Antennas and Propagation*, Vol. 43, No. 6, pp. 627-629, June, 1995.

[10] P.T. Lam, S. Lee, D.C.D. Chang, and K.C. Lang. Directivity Optimization of a Reflector Antenna with Cluster Feeds: A Closed-Form Solution. *IEEE Transactions on Antennas and Propagation*, Vol. 33, No. 11, pp.1163-1473, November, 1985.

[11] Y. Rahat-Samii and S. Lee. Directivity of Planar Array Feeds for Satellite Reflector Applications. *IEEE Transactions on Antennas and Propagation*, Vol. 31, No. 3, pp. 463-470, May, 1983.

[12] C.C. Hung and R. Mittra. Secondary Pattern and Focal Region Distribution of Reflector Antennas Under Wide-Angle Scanning. *IEEE Transactions on Antennas and Propagation*, Vol. 31, No. 5, pp. 756-763, September, 1983.

[13] V. Galindo-Israel, S. Lee and R. Mittra. Synthesis of a Laterally Displaced Cluster Feed for a Reflector Antenna with Application to Multiple Beams and Contoured Patterns. *IEEE Transactions on Antennas and Propagation*, Vol. 26. No. 2, pp. 220-228, March, 1978.

[14] S. Lee and Y. Rahmat-Samii. Simple Formulas for Designing an Offset Multibeam Parabolic Reflector. *IEEE Transactions on Antennas and Propagation*, Vol. 29, No. 3, pp. 472-478, May, 1981.

[15] A.R. Cherrette, R.J. Acosta, P.T. Lam, and S. Lee. Compensation of Reflector Antenna Surface Distortion Using an Array Feed. *IEEE Transactions on Antennas and Propagation*, Vol. 37, No. 8, pp. 966-978, August, 1989.

[16] A.W. Rudge and N.A. Adatia. Offset-Parabolic-Reflector Antennas: A Review. *IEEE Proceedings*, Vol. 66, No. 12, pp. 1592-1618, December, 1978.

[17] Y. Rahmat-Samii and V. Galindo-Israel. Shaped Reflector Antenna Analysis Using the Jacobi-Bessel Series. *IEEE Transactions on Antennas and Propagation*, Vol. 28, No. 4, pp. 425-435, July, 1980.

[18] Y. Rahmat-Samii, P. Cramer, Jr., K. Woo, and S. Lee. Realizable Feed-Element Patterns for Multibeam Reflector Antenna Analysis. *IEEE Transactions on Antennas and Propagation*, Vol. 29, No. 6, pp.961-963, November, 1981.

[19] S.H. Stewart and W.L. Stutzman. Analysis of Reflector Antenna Systems with Arbitrary Feed Arrays Using Primary Field Superposition. *IEEE Transactions on Antennas and Propagation*, Vol. 38, No. 7, pp. 994-1000. July, 1990.

[20] R. Mittra, W.L. Ko, and M.S. Sheshadri. A Transform Technique for Computing the radiation Pattern of Prime-Focal and Cassegrainian Reflector Antennas. *IEEE Transactions on Antennas and Propagation*, Vol. 30, No. 3, pp. 520-524, May, 1982.

[21] G. Franceschetti and A. Mohsen. Recent Developments in the Analysis of Reflector Antennas. A Review. *IEEE Proceedings*, Vol. 133, No. 1, pp. 65-76, February, 1986.

[22] Y. Rahmat-Samii. Useful Coordinate Transformations for Antenna Applications. *IEEE Transactions on Antennas and Propagation*, Vol. 27, No. 4, pp. 571-574, July, 1979.

[23] P.T. Lam. On the Calculation of the Directivity of Planar Array Feeds for Satellite Reflector Applications. *IEEE Transactions on Antennas and Propagation*, Vol. 33, No. 5, p. 571, May, 1985.

[24] R. Mittra, Y. Rahmat-Samii, V. Galindo-Israel, and R. Norman. An Efficient Technique for the Computation of Vector Secondary Patterns of Offset Paraboloid Reflectors. *IEEE Transactions on Antennas and Propagation*, Vol. 27, No. 3, pp. 294-304, May, 1979.

[25] V. Galindo-Israel and R. Mittra. A New Series Representation for the Radiation Integral with Application to Reflector Antennas. *IEEE Transactions on Antennas and Propagation*, Vol. 25, No. 5, pp. 631-641, September, 1977.

[26] H. Steyskal. Digital Beamforming Antennas. *Microwave Journal*, pp. 107-124, January, 1987.

[27] W.D. Ivancic, M.J. Shalkhauser, and J.A. Quintana. A Network Architecture for a Geostationary Communication Satellite. *IEEE Communications Magazine*, pp. 72-84, July, 1994.

[28] A.D. Craig, C.K. Leong, and A. Wishart. Digital Signal Processing in Communications Satellite Payloads. *Electronics Communication Engineering Journal*, Vol. 4, No. 3, June, 1992.

[29] W.A. Gardner, S.V. Schell and P.A. Murphy. Multiplication of Cellular Radio Capacity by Blind Adaptive Spatial Filtering. In *Proceedings of the International Conference on Selected Topics in Wireless Communications*, pp. 102-106, 1992.

[30] W.A. Gardner. *Statistical Spectral Analysis: A Non-Probabilistic Theory.* Prentice-Hall, Englewood Cliffs, NJ, 1987.

[31] W.A. Gardner, editor. *Cyclostationarity in Communications and Signal Processing.* IEEE Press, New York, NY, 1994.

[32] B.G. Agee, S.V. Schell, and W.A. Gardner. Spectral self-coherence restoral: a new approach to blind adaptive signal extraction using antenna arrays. *IEEE Proceedings*, Vol. 78, No. 4, pp. 753-767, April 1990.

[33] W.A. Gardner. Cyclic Wiener filtering: theory and method. *IEEE Transactions on Communications*, Vol. 41, No. 1, pp. 151-163, January 1993.

[34] W.A. Gardner. Spectral correlation of modulated signals: Part I - Analog modulation. *IEEE Transactions on Communications*, Vol. 35, No. 6, pp. 584-594, June 1987.

[35] W.A. Gardner, W.A. Brown, and C.-K. Chen. Spectral correlation of modulated signals: Part II - Digital Modulation. *IEEE Transactions on Communications*, Vol. 35, No. 6, pp. 595-601, June 1987.

[36] W.A. Gardner. The spectral correlation theory of cyclostationary time-series. *Signal Processing*, Vol. 11, pp. 13-36, July 1986.

[37] L. Castedo, and A.R. Figueiras-Vidal. An adaptive beamforming technique based on cyclostationary signal properties. *IEEE Transactions on Signal Processing*, Vol. 43, No. 7, pp. 1637-1650, July 1995.

[38] W.A. Gardner. Exploitation of spectral redundancy in cyclostationary signals. *IEEE Signal Processing Magazine*, pp. 14-36, April 1991.

[39] Q. Wu, and K.M. Wong. Adaptive beamforming of cyclic signal and fast implementation. In *IEEE International Conference on Acoustics, Speech and Signal Processing*, Vol. IV, pp. 157-160, 1994.

[40] Q. Wu, K.M. Wong, and R. Ho. Fast algorithm for adaptive beamforming of cyclic signals. *IEE Proceedings on Radar, Sonar and Navigation*, Vol. 141, No.6, pp.312-318, December 1994.

[41] J.T. Mayhan and L. Niro. Spatial Spectral Estimation Using Multiple Beam Antennas. *IEEE Transactions on Antennas and Propagation*, Vol. Ap-35, No. 8, August 1987.

[42] G.G. Chadwick et al. Adaptive Antenna/Receiver-Processor System. *1981 International Symposium Digest, Antennas and Propagation*, Vol. 1, pp. 272-275, 1981.

[43] J.W. Cofer, G.P. Martin, S.E. Ralph. Adaptive Null Steering By Reflector Antennas. In *Proceedings of the 2nd International Conference on Antennas and Propagation*, York, England, pp. 169-173, 1981.

[44] J.T. Mayhan. Area Coverage Adaptive Nulling From Geosynchronous Satellites: Phased Arrays Versus Multiple-Beam Antennas. *IEEE Transactions on Antennas and Propagation*, Vol. AP-34, No. 3, pp. 410-419, March 1986.

[45] K.M. Soo Hoo, and R.B. Dybdal. Adaptive Multiple Beam Antennas for Communications Satellites. In *Proceedings of the 1990 International IEEE/AP-S Symposium*, pp. 1880-1883, May 1990.

[46] K. Sudhakar Rao et al. Development of a 45 GHz Multiple-Beam Antenna for Military Satellite Communications. *IEEE Transactions On Antennas and Propagation*, Vol. 43, No. 10, October 1995.

[47] R.A. Shore. Adaptive Nulling in Hybrid Reflector Antennas. *Rome Laboratory - In-House Report*, September 1992.

[48] W.H. Press et al. *Numerical Recipes in C: The Art of Scientific Computing, 2nd Edition*. Cambridge University Press, New York, NY, 1992.

[49] R.T. Compton, Jr. *Adaptive Antennas: Concepts and Performance*. Prentice Hall, Englewood Cliffs, NJ, 1988.

[50] C. Scott. *Modern Methods of Reflector Antenna Analysis and Design*. Artech House, Boston, 1990.

[51] G. Maral, and M. Bousquet. *Satellite Communications Systems, 2nd Edition*. John Wiley & Sons, Toronto, 1993.

[52] A.W. Love, editor. *Reflector Antennas*. IEEE Press, New York, NY, 1978.

[53] R.A. Monzingo, and T.W. Miller. *Introduction to Adaptive Arrays*. John Wiley & Sons, Toronto, 1980.

[54] A.M. Parolin. *Performance of Adaptive Antenna Arrays in a Fast Packet Network*. M.Sc. thesis, Department of Electrical and Computer Engineering, Queen's University, Kingston, Ont., 1994.

[55] Y.T. Lo, and S.W. Lee, editors. *Antenna Handbook: Theory, Applications, and Design*. Van Nostrand Reinhold Company, New York, NY, 1988.

[56] A.D. Olver et al. *Microwave Horns and Feeds*. IEEE Press, England, 1994.

[57] S. Haykin. *Adaptive Filter Theory*. Prentice Hall, Englewood Cliffs, NJ, 1986.

[58] J.D. Kraus. *Antennas, 2nd edition.* McGraw-Hill Book Company, Toronto, 1988.

[59] S. Silver, editor. *Microwave Antenna Theory and Design.* Peter Peregrinus Ltd., London, UK, 1984.

[60] H. Goldstein. *Classical Mechanics.* Addison-Wesley, Reading, MA, 1953.

[61] J. Karimi. *Personal Hand-Held Communications Via L-Band CDMA-Based Geostationary Beamforming Satellites.* M.Sc. thesis, Department of Electrical and Computer Engineering, Queen's University, Kingston, Ont., Feb. 1996.

[62] R.O. Schmidt. *A Signal Subspace Approach to Multiple Emitter Location and Spectral Estimation.* PhD thesis, Stanford University, Standford, CA, Nov. 1981.

[63] R.F. Harrington. *Time-Harmonic Electromagnetic Fields.* McGraw-Hill Book Company, Toronto, 1961.

[64] R.E. Colin, and F.J. Zucker, editors. *Antenna Theory: Part 1.* McGraw-Hill Book Company, Toronto, 1969.

[65] A. Jeffrey. *Handbook of Mathematical Formulas and Integrals.* Academic Press, Toronto, 1995.

[66] M. Abramowitz, and I.A. Stegun, editors. *Handbook of Mathematical Functions.* Dover Publications, New York, 1965.

[67] J. Duggan. *Adaptive Beamforming with a Focal-Fed Offset Parabolic Reflector Antenna.* Master's thesis, Dept. of Electrical and Computer Engineering, Queen's University, Kingston, ON, 1997.

[68] Jack H. Winters, Jack Salz, and Richard D. Gitlin. "The impact of antenna diversity on the capacity of wireless communication systems". *IEEE Transactions on Communications,* 42(2/3/4): 1740-1751, 1994.

DATE DUE
DATE DE RETOUR
